Multi-Tier and Multi-Bit Reversible Data Hiding with Contents Characteristics

Hsiang-Cheh Huang

Department of Electrical Engineering
National University of Kaohsiung
700 University Road, Kaohsiung 811, Taiwan, R.O.C.
hch.nuk@gmail.com

Feng-Cheng Chang*

Department of Innovative Information and Technology
Tamkang University
180 Linwei Road, Jiaosi, Ilan 262, Taiwan, R.O.C.
* : Corresponding author.
135170@mail.tku.edu.tw

ABSTRACT. *Reversible data hiding, also known as lossless data hiding, is a newly developed research field and relating applications in digital rights management (DRM). With the widespread use of tablets or smart phones, digital images are captured and shared online instantly. Therefore, the ownership of the images taken has become an important issue in this field. With reversible data hiding, secret information can be hidden into the original image at the encoder, and then the image containing secret data, or the marked image, is delivered to the decoder. For decoding, in order to meet the requirement of reversibility, original image and secret information need to be perfectly separated from the marked image. By modifying difference values corresponding to the characteristics of original image, and by use of multi-tier embedding, the larger amount of secret information can be embedded at the encoder. Later on, with the reasonable size of side information, both the original image and the secret information can both be separated at the decoder. We take the relationships between adjacent pixels into consideration, and propose the multi-bit embedding scheme that is able to hide more than one bit per pixel of data capacity, with the reasonable output image quality. Simulation results with our algorithm have demonstrated the better results over existing ones for practical applications. With the comparisons of embedding capacity for encoding, and side information for decoding, our algorithm works well under the requirement of high data capacity for reversible data hiding.*

Keywords: Reversible data hiding, Image quality, Multi-bit embedding, Capacity, Side information.

1. **Introduction.** With the widespread use of tablets or smart phones in our daily lives, digital images are captured and shared online instantly. Therefore, the ownership of the images taken has become an important issue in this field. For ownership protection of multimedia contents, by use of encryption or watermarking have demonstrated the effectiveness for this kind of applications [1, 2]. In recent years, reversible data hiding has drawn attention to researchers in watermarking and digital rights management (DRM) systems [3, 4]. For conventional data hiding or watermarking applications, at the encoder,

the secret information can be embedded into the original images by use of algorithms designed by researchers, and then the image containing hidden data can be transmitted to the receiver. After reception of the marked media, only the secret information need to be extracted, and the ownership of such media can be authenticated [5, 6]. Different from conventional watermarking applications, for reversible data hiding, while decoding, both the original image, and the hidden data embedded into the image, need to be recovered and extracted perfectly [7, 8, 9]. Therefore, evaluation of reversible data hiding algorithms would be somewhat different from conventional viewpoints [10, 11].

In this paper, we focus on the algorithm development for reversible data hiding [12, 13]. It means that the hidden secret can be embedded into the original image by algorithms at the encoder. It would be much required to take advantage of the inherent characteristics of original images into consideration in order to look for better performances [14, 15]. At the decoder, with the aid of side information provided, the original image and the hidden data can both be perfectly recovered [16, 17]. Considering the characteristics of original images [18, 19], we propose the multi-tier and multi-bit embedding algorithm for reversible data hiding. When embedding multiple bits at once for several times, considerable increase in the size of secret information can be expected. Researchers have proposed the concepts for embedding multiple bits at a time to gain increased amounts for embedding [20]. On the contrary, more amounts of bits embedded implies more degradation to the image quality. How to effectively choose the balance between the two would be of great interest.

With our algorithm, we can embed the more number of bits into the original image, with the acceptable quality of the output image. The reasonable amount of side information for decoding can be obtained. Most important of all, the hidden data and original image can perfectly be recovered, and the reversible property can be reached. Simulation results have demonstrated these observations.

This paper is organized as follows. In Sec. 2, we discuss about the parameters for accessing the reversible data hiding algorithm. In Sec. 3, we present the proposed algorithm. Simulation results are demonstrated in Sec. 4, which point out the more embedding capacity with the acceptable image quality. Finally, we conclude this paper in Sec. 5.

2. **Parameters for Accessing Reversible Data Hiding Algorithms.** There are lots of parameters for accessing how effective the reversible data hiding algorithms are. These include the capacity for data embedding, the imperceptibility or the output image quality, and the side information for decoding. Most important of all, the reversibility of the algorithm should be retained at the decoder. Before going into more details of the parameters, we first address the practical algorithms for reversible data hiding. There are two major classes for making reversible data hiding possible. These are the histogram-based algorithms [12, 13], and the difference expansion (DE) algorithms [14, 15]. For the former class, the global characteristics of original image are considered. For the latter one, characteristics among neighboring pixels are taken into account. Discussions about these parameters are stated as follows.

2.1. **The Embedding Capacity.** The capacity for data embedding, represented by bit per pixel (bit/pixel, or bpp), is the ratio between the number of bits of secret information and the number of pixels of the original image. On the one hand, with the histogram-based scheme [12, 13], the capacity is limited by the peak point in the histogram, implying very low capacity for embedding. On the other hand, with the difference expansion scheme [14, 15], one bit can be embedded into two consecutive pixels (or a pair of pixels), implying the capacity of 0.5 bpp. Thus, 0.5 bpp can be considered as the benchmark for accessing the performance in embedding capacity.

Generally speaking, the more embedding capacity would be expected by users. However, more embedding bits imply more alteration to the original image, causing the degradation of output image quality. Thus, how to increase the maximally allowable capacity, and then to control the number of embedding bits for keeping the acceptable imperceptibility and corresponding performances of the algorithm, are the goals for the design of algorithm.

2.2. **The Imperceptibility.** The imperceptibility denotes the quality of image after data embedding. We use the peak signal-to-noise ratio (PSNR) to represent imperceptibility of output image. The higher PSNR value implies the better imperceptibility. With the histogram-based scheme, the output PSNR of at least 48.13 dB is guaranteed [12]. With the difference expansion scheme, due to the mass amount of capacity embedded, the degradation of quality would be expected.

2.3. **The Side Information.** The two classes of algorithms lead to different amount of side information. Firstly, with the histogram-based algorithm, the luminance value denoting the peak of histogram, which is one byte, would be necessary for decoding [12, 13]. Secondly, with the DE scheme, if the luminance values between two consecutive pixels differ too much, it will cause the overflow problem [14, 15]. Under this condition, coordinates of pixel locations should be recorded, denoting the positions unable for embedding. These coordinates are called the location map. For most images, the size of the location map is large. Thus, how to use a small amount of side information for reversible data hiding is a challenging task.

2.4. **The Reversibility.** The most important factor for reversible data hiding is that the algorithm needs to be *reversible*. That is, with the necessary side information, both the original image and the hidden secret need to be perfectly reconstructed at the decoder.

3. **Proposed Algorithm.** Here we propose our algorithm for multi-level data embedding. Based on the concepts and corresponding modifications from [12, 13] and [14, 15], the more embedding capacity can be obtained with the acceptable output quality.

3.1. **Using the S-shape Scanning.** It is easily observed that neighboring pixels in spatial locations tend to have similar luminance values. We can try to embed the data bits by modifying the luminance values among pixels. As an example in Fig. 1, the 3×3 test image in Fig. 1(a) can be scanned by following the order with the arrows in Fig. 1(b). It can then turn into the 1×9 array with the snake-shape scanning (S-scanning) [21, 22] as depicted in Fig. 1(c).

Let the original image be $\boldsymbol{X}$ with size $M \times N$. With the S-scanning scheme, $\boldsymbol{X}$ will turn into the 1-D array, represented by $\boldsymbol{P} = \{p_1, p_2, \cdots, p_{m \times n}\}$.

3.2. **Calculation of the Difference.** Based on the histogram-based scheme [12], embedding capacity is limited by the peak point of the histogram. By calculating the difference between the neighboring elements in $\boldsymbol{P}$, more capacity can be expected because of the high peak around zero. The array relating to the difference, $\boldsymbol{D} = \{d_1, d_2, \cdots, d_{m \times n}\}$, can be calculated with Eq. (1). We keep the initial pixel intact, and take the difference values between neighboring elements in the 1-D array.

$$d_i = \begin{cases} p_i, & i = 1; \\ p_{i-1} - p_i, & i = 2, 3, \cdots, m \times n. \end{cases} \tag{1}$$

Figure 2 is the depiction of the histogram with Eq. (1) for the test image `Lena`. The peak point with the difference histogram is 10.16 times larger than its original counterpart.

a	b	c
d	e	f
g	h	i

(a)

a	b → c
d	e f
g → h	i

(b)

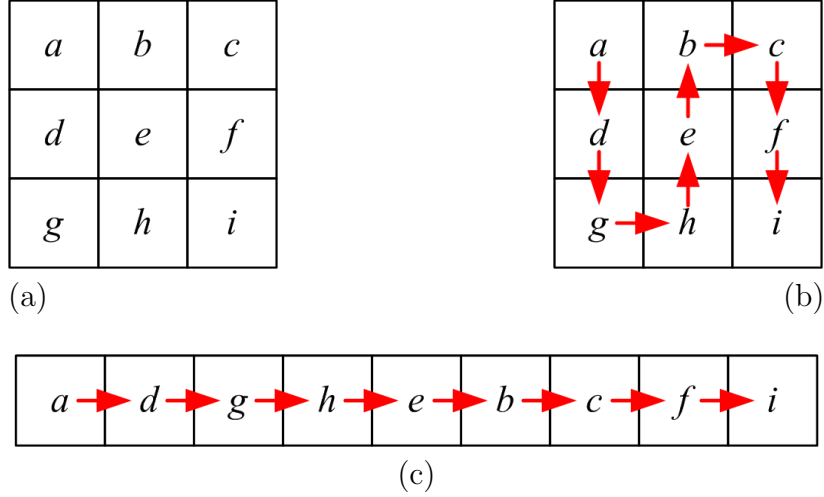| a →	d →	g →	h →	e →	b →	c →	f →	i

(c)

FIGURE 1. Demonstration of S-shape scanning. (a) The original 3×3 image. (b) The S-scanned image with the arrows for reference. (c) The 1×9 image corresponding to the original image.
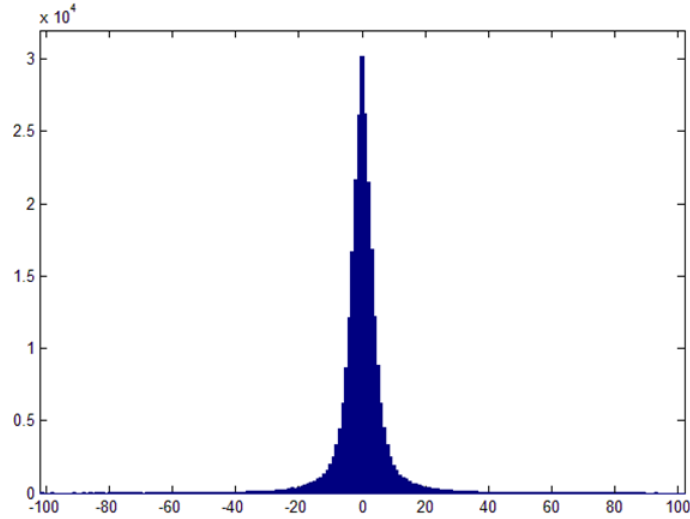

FIGURE 2. The histogram of the difference values between adjacent pixels with Eq. (1) for the Lena image.

3.3. **Data Embedding.** For embedding the secret information, we first determine the embedding level (EL), which is a positive integer, for the possible locations to hide the secret. The EL value also influences the embedding capacity and marked image quality. Next, the following steps are performed sequentially for data embedding.

Step 1: For EL with values of 0 and 1, conditions for the new difference value d_i' in Eq. (2) should be satisfied to meet Step 2.

$$d_i' = \begin{cases} d_i, & \text{if } i = 1; \\ d_i, & \text{if } d_i = -1 \text{ or } 0, \quad i = 2, 3, \cdots, m \times n; \\ d_i - 1, & \text{if EL} \leq -1, \qquad i = 2, 3, \cdots, m \times n; \\ d_i + 1, & \text{if EL} \geq 1, \qquad i = 2, 3, \cdots, m \times n. \end{cases} \tag{2}$$

Step 2: According to the capacity for embedding, based on the difference values in Fig. 2 for preliminary prediction, the corresponding EL can be determined with
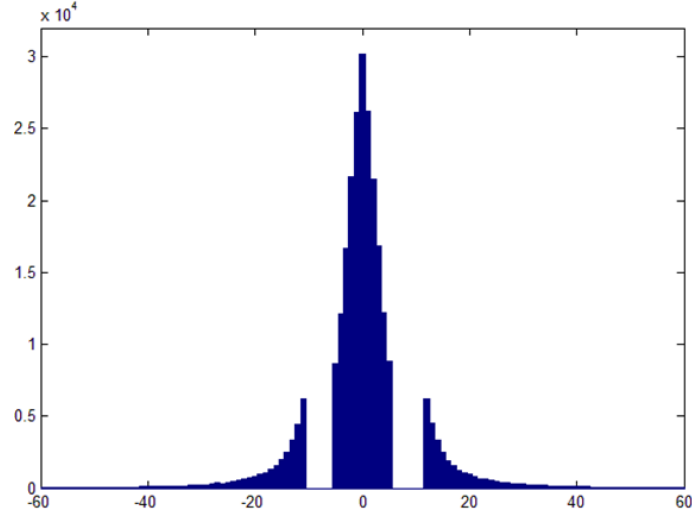
FIGURE 3. Operations of bins emptying with EL $= 5$ for `Lena`.
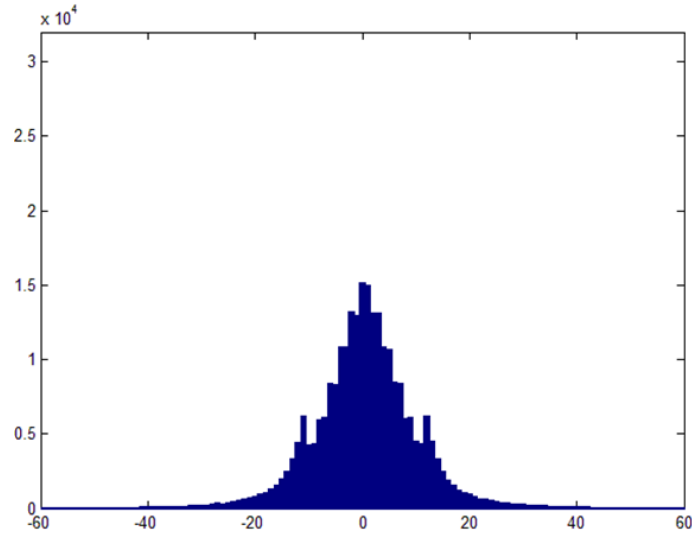
FIGURE 4. Operations of secret embedding with EL $= 5$ for `Lena`.

Eq. (3), and Fig. 3 is an example for EL $= 5$. When we make comparisons between Fig. 2 and Fig. 3, we observe that some difference values are intentionally left blank for data embedding.

$$d_i'' = \begin{cases} d_i', & \text{if } i = 1; \\ d_i', & \text{if } -\text{EL} \leq d_i' \leq \text{EL}, & i = 2, 3, \cdots, m \times n; \\ d_i' - \text{EL} - 1, & \text{if } d_i' < -\text{EL}, & i = 2, 3, \cdots, m \times n; \\ d_i' + \text{EL}, & \text{if } d_i' > \text{EL}, & i = 2, 3, \cdots, m \times n. \end{cases} \tag{3}$$

Step 3: We employ the multi-tier embedding to look for enhanced capacity for embedding. Two sets of secret data are prepared for embedding, with the binary representation of the single-bit secret information $W_1 \in \{0, 1\}$, and the double-bit secret information $W_2 \in \{00, 01, 10, 11\}$. W_1 is going to be embedded into the range between –EL and EL in the difference histogram. Embedding can be performed with Eq. (4) until EL$= -2$ or EL$= 3$. Fig. 4 depicts an example for EL $= 5$ after secret

embedding.

$$
d_i''' =
\begin{cases}
d_i'', & \text{if } i = 1; \\
d_i'', & \text{if } -\text{EL} < d_i'' < \text{EL}, & i = 2, 3, \cdots, m \times n; \\
2 \cdot \text{EL} - W_1, & \text{if } d_i'' = -\text{EL}, \ \text{EL} \neq 0, & i = 2, 3, \cdots, m \times n; \\
2 \cdot \text{EL} + W_1 - 1, & \text{if } d_i'' = \text{EL}, \ \text{EL} \neq 0 \text{ or } 1, & i = 2, 3, \cdots, m \times n.
\end{cases}
\tag{4}
$$

Next, W_2 is going to be embedded with Eq. (5).

$$
d_i''' =
\begin{cases}
d_i'', & \text{if } i = 1; \\
d_i'', & \text{if } \text{EL} > 1 \text{ or } \text{EL} < 0, & i = 2, 3, \cdots, m \times n; \\
4 \cdot \text{EL} - W_2, & \text{if } \text{EL} = 0 \text{ or } 1, & i = 2, 3, \cdots, m \times n.
\end{cases}
\tag{5}
$$

When we make comparisons between Fig. 3 and Fig. 4, we observe that after the multi-tier and multi-bit data embedding, the peak in Fig. 4 has become lowered to compare to the peak in Fig. 3.

Step 4: Obtain the output image. First, the 1-D output can be calculated with Eq. (6).

$$
p_i' =
\begin{cases}
p_i, & i = 1; \\
p_{i-1} - d_i''', & i = 2, 3, \cdots, m \times n.
\end{cases}
\tag{6}
$$

Hence, $\boldsymbol{P'} = \{p_1', p_2', \cdots, p_{m \times n}'\}$. Next, with the inverse S-scanning, the 2-D output image, $\boldsymbol{X'}$, can be acquired.

Figure 5 is an illustration for the embedding procedures with Fig. 1(a). For simplicity, we use the matrix to present the relationships between Fig. 1(a) and Figure 5 as below:

$$
\begin{bmatrix}
a & b & c \\
d & e & f \\
g & h & i
\end{bmatrix}
=
\begin{bmatrix}
60 & 68 & 64 \\
64 & 70 & 66 \\
63 & 64 & 66
\end{bmatrix}.
$$

3.4. **Data Extraction and Original Recovery.** At the decoder, data extraction and image recovery would be the reverse operation to its embedding counterpart. With the reasonable amount of side information, original image can be reconstructed and secret data can be extracted. The following steps are performed subsequently at the decoder.

Step 1: We perform the S-scanning for the received image $\boldsymbol{X'}$ with Fig. 1(b), and get $\boldsymbol{P'} = \{p_1', p_2', \cdots, p_{m \times n}'\}$.

Step 2: The difference values between adjacent elements in $\boldsymbol{P'}$ are calculated, and δ_i are obtained in Eq. (7).

$$
\delta_i =
\begin{cases}
p_i', & i = 1; \\
p_{i-1} - p_i', & i = 2, 3, \cdots, m \times n.
\end{cases}
\tag{7}
$$

Step 3: With the received side information EL, the bit values of the single-bit information in $W_1' = \{0, 1\}$ can be extracted with Eq. (8).

$$
W_1' =
\begin{cases}
0, & \text{if } \delta_i = (2 \cdot \text{EL} + 1) \text{ or } (-2 \cdot \text{EL}); \\
1, & \text{if } \delta_i = (2 \cdot \text{EL}) \text{ or } (-2 \cdot \text{EL} - 1).
\end{cases}
\tag{8}
$$

Step 4: The difference values in the recovered image, for $i = 2, 3, \cdots, m \times n$, can be obtained with Eq. (9).

$$
\delta_i' =
\begin{cases}
\delta_i - \text{EL} - 1, & \text{if } \delta_i > 2 \cdot \text{EL}; \\
\delta_i + \text{EL} + 2, & \text{if } \delta_i < -2 \cdot \text{EL} - 1; \\
r - 1, & \text{if } \delta_i = 2r - 1 \text{ or } 2r, & r = 3, 4, \cdots, \text{EL}; \\
-r + 1, & \text{if } \delta_i = -2r - 1 \text{ or } -2r, & r = 2, 3, \cdots, \text{EL}.
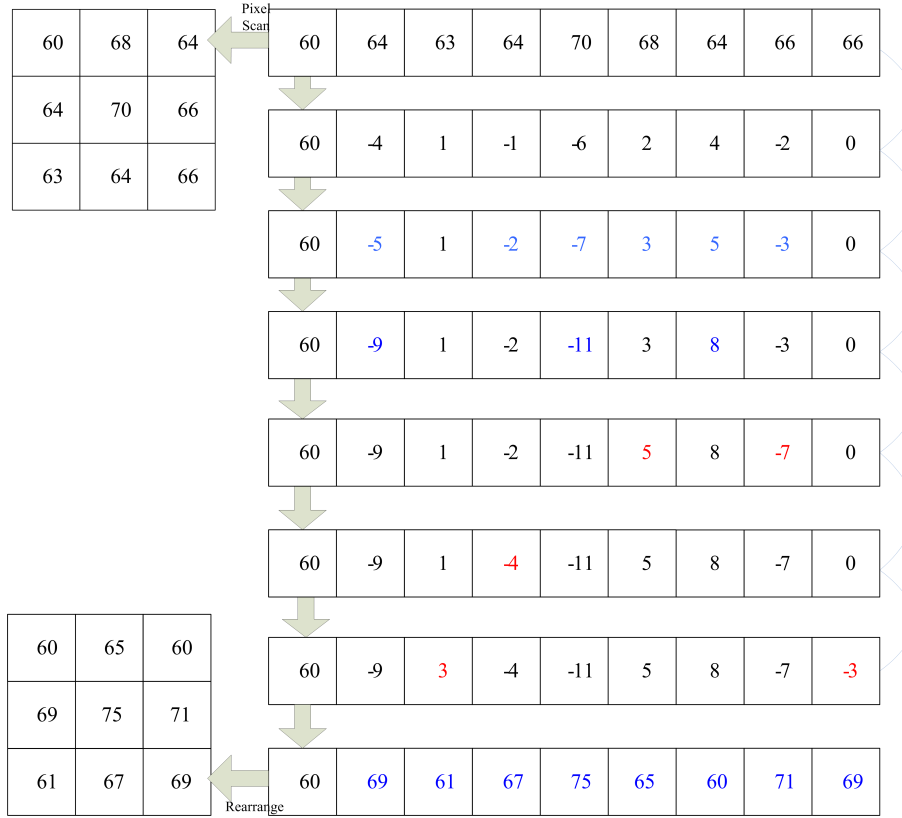\end{cases}
\tag{9}
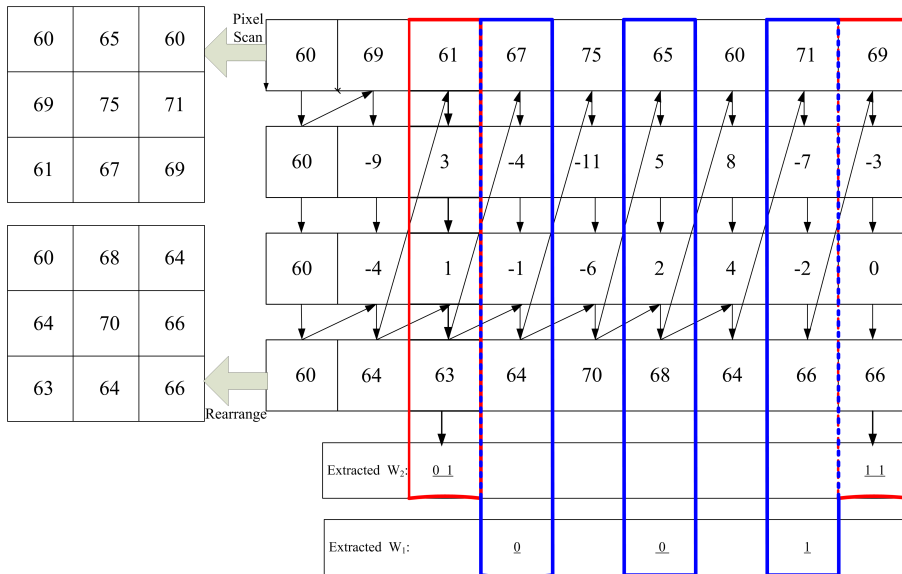$$

FIGURE 5. Illustration of the embedding procedure.

FIGURE 6. Illustration of the embedding procedure.

Step 5: The double-bit information $W_2' = \{00, 01, 10, 11\}$ can be calculated by

$$\delta_i'' = \left\lceil \frac{1}{4}\delta_i \right\rceil. \tag{10}$$

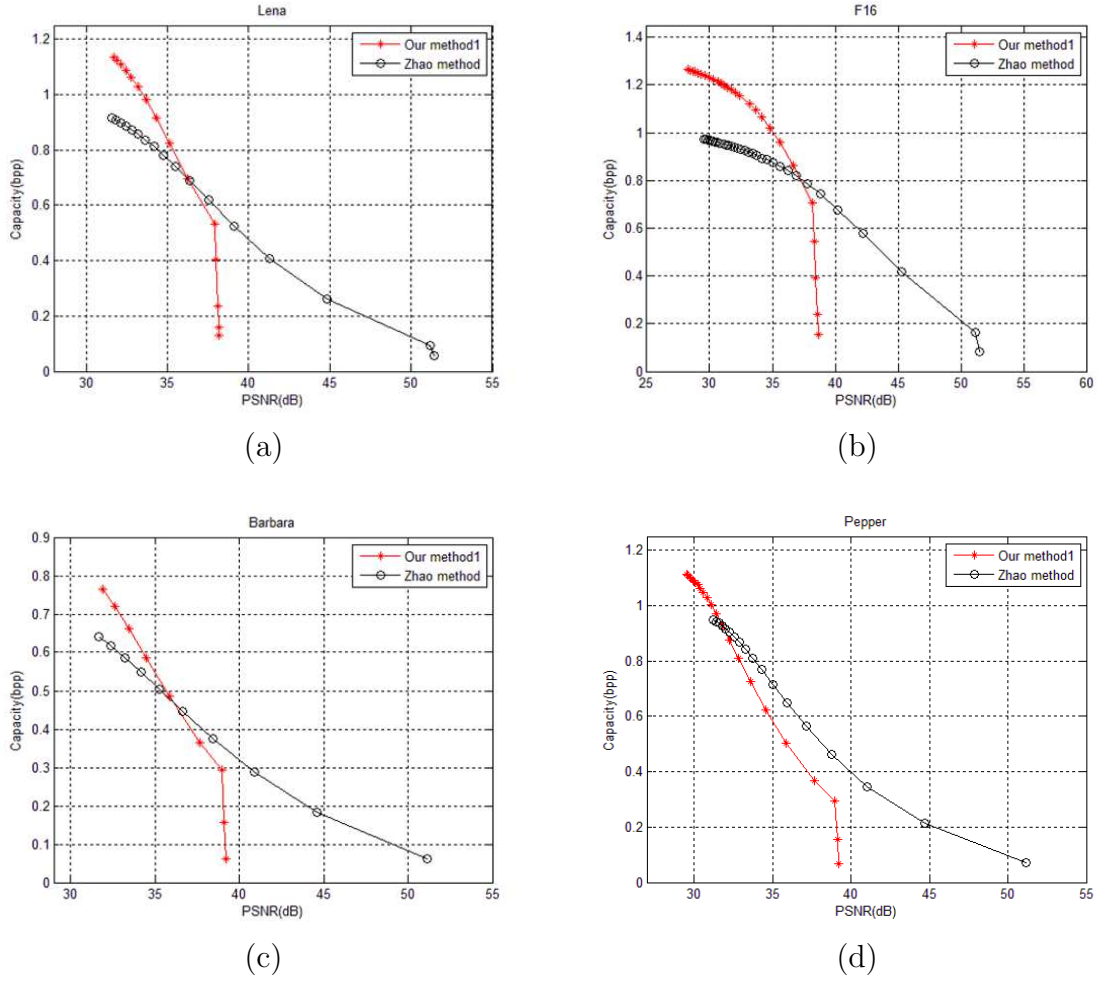$$W_2' = |\delta_i - 4 \cdot \delta_i''|. \tag{11}$$

FIGURE 7. Comparisons between capacity and PSNR with (a) `Lena`, (b) `F16`, (c) `Barbara`, and (d) `pepper`. More than 1.0 bpp can be obtained with our scheme.

Step 6: With the difference values, the 1-D array, $\boldsymbol{P''}$, can be reconstructed with Eq. (12).

$$p_i'' = \begin{cases} p_i, & i = 1; \\ p_{i-1}' + \delta_i'', & i = 2, 3, \cdots, m \times n. \end{cases} \tag{12}$$

Step 7: Applying the inverse S-scanning to $\boldsymbol{P''}$, recovered image, $\boldsymbol{X''}$, should be identical to its counterpart, $\boldsymbol{X}$.

In conjunction with Fig. 5, Fig. 6 is a demonstration for data extraction and original recovery with Fig. 1(a).

4. **Simulation Results.** In our simulations, we choose the test images with the picture sizes of 512×512, for conducting simulations. The secret information W_1 and W_2 to be hidden are randomly generated bitstreams. We also record the maximally allowable capacity for the test images. From Fig. 7, comparisons about the performances between the marked image quality and the embedding capacity for `Lena`, `F16`, `Barbara`, and `pepper` are presented. Comparisons to Zhao *et al.*'s method in [13] are also provided. We skip to compare to conventional schemes in [12] and [14] due to the limited amounts of capacity that can be offered.

TABLE 1. Comparisons of maximally allowable capacities and output image quality. all images have sizes of 512×512.

Image	Our Scheme		Relating Scheme in [13]	
	Capacity (bpp)	Output PSNR (dB)	Capacity (bpp)	Output PSNR (dB)
Barbara	0.800	31.25	0.662	31.05
F16	1.266	28.30	0.974	29.57
Goldhill	0.770	32.57	0.749	31.72
Jet	1.333	34.40	0.963	37.68
Lena	1.135	31.68	0.916	31.58
Tank	0.805	32.71	0.789	30.96

Regarding to the performance comparisons, we first take the embedding capacity for comparisons. We observe our scheme has the ability to embed more than 1.0 bpp of capacity with the results presented in Fig. 7, meaning the number of embedded bits is larger than the size of original image due to the multi-tier and multi-bit embedding. Performance curves with our method generally outperform those with [13] as depicted in Figs. 7(a), (b), and (c) for Lena, F16, and Barbara, respectively. For the results in Fig. 7(d) for pepper, they generally perform inferior with our method except for the portion for embedding large amounts of capacity. This may due to the inherent characteristics of original image, and the prevention of location map that may limit upper bound of the EL value, and hence the reduction of effective capacity.

Finally, the maximally allowable capacities for the six test images with sizes of 512×512 are looked for. Comparisons between capacity and output PSNR are represented in Table 1. Due to different characteristics of test images, even though multi-bit embedding is applied, capacity of more than 1.0 bpp can be obtained for part of the image. And more capacity can be embedded over conventional scheme [13].

Regarding to the side information with our method, only the EL value is required, and no location map is needed. With our method, for the generation of difference values before embedding, we first check the largest and the smallest values in the difference histogram. The portion between the largest value and 255, and between the smallest one and –255, are checked in advance. The EL value is chosen to prevent from the overflow problem after data embedding, and hence no location map would be produced. Thus, EL plays the key role for reversible data decoding.

5. **Conclusions.** In this paper, we focus on the characteristics of original image, and propose the multi-tier and multi-bit reversible data hiding algorithm with the capability for embedding high capacity. The maximal number of bits has the potential to surpass 1.00 bpp, meaning that the size of secret data, represented by bits, can be larger than the size of the original image. Before the embedding of secret information, the EL value is carefully selected to prevent from the generation of location map. Under these conditions, the quality of marked image is acceptable both objectively and subjectively. With the reasonable amount of side information, or the embedding level, both the original image and the secret data can be perfectly recovered, and hence the reversibility of our scheme can be guaranteed. We are going to improve our scheme for the range of low embedding capacity, and make the output image quality to be comparable to those with existing schemes.

REFERENCES

[1] H. C. Huang, F. C. Chang, Y. H. Chen, and S. C. Chu, "Survey of bio-inspired computing for information hiding," *J. Information Hiding and Multimedia Signal Processing*, vol. 6, no. 3, pp. 430–443, May 2015.

[2] Y. H. Chen and H. C. Huang, "Coevolutionary genetic watermarking for owner identification," *Neural Computing and Applications*, vol. 26, no. 2, pp. 291–298, Feb. 2015.

[3] C. C. Lai, H. C. Huang and C. C. Tsai, "Image watermarking scheme using singular value decomposition and micro-genetic algorithm," *Proc. IIHMSP'08*, pp. 469–472, 2008.

[4] H. C. Huang, Y. H. Chen, and A. Abraham, "Optimized watermarking using swarm-based bacterial foraging," *J. Inf. Hiding and Multimedia Signal Proc.*, vol. 1, no. 1, pp. 51–58, Jan. 2010.

[5] H. C. Huang and F. C. Chang, "Robust image watermarking based on compressed sensing techniques," *J. Inf. Hiding and Multimedia Signal Proc.*, vol. 5, no. 2, pp. 275–285, Apr. 2014.

[6] H. C. Huang and W. C. Fang, "Metadata-based image watermarking for copyright protection," *Simulation Modelling Practice and Theory*, vol. 18, no. 4, pp. 436–445, Apr. 2010.

[7] B. Yan, Y. F. Wang, L. Y. Song, and H. M. Yang, "Power spectrum compliant QIM watermarking for autoregressive host signals," *J. Inf. Hiding and Multimedia Signal Proc.*, vol. 6, no. 5, pp. 882–888, Sep. 2015.

[8] H. C. Huang and F. C. Chang, "Hierarchy-based reversible data hiding," *Expert Systems with Applications*, vol. 40, no. 1, pp. 34–43, Jan. 2013.

[9] H. C. Huang and W. C. Fang, "Techniques and applications of intelligent multimedia data hiding," *Telecommunication Systems*, vol. 44, no. 3-4, pp. 241–251, Aug. 2010.

[10] S. W. Weng and J. S. Pan, "Reversible watermarking based on multiple prediction modes and adaptive watermark embedding," *Multimedia Tools and Applications*, vol. 72, no. 3, pp. 3063–3083, Oct. 2014.

[11] S. W. Weng, Y. Zhao, R. R. Ni, and J. S. Pan, "Parity-invariability-based reversible watermarking," *Electronics Letters*, vol. 45, no. 20, pp. 1022–1023, Sep. 2009

[12] Z. Ni, Y. Q. Shi, N. Ansari, and W. Su, "Reversible data hiding," *IEEE Trans. Circuits Syst. Video Technol.*, vol. 16, no. 3, pp. 354–362, Mar. 2006.

[13] Z. Zhao, H. Luo, Z. M. Lu, and J. S. Pan, "Reversible data hiding based on multilevel histogram modification and sequential recovery," *AEU — Int'l J. Electron. Commun.*, vol. 65, pp. 814–826, Oct. 2011.

[14] J. Tian, "Reversible data embedding using a difference expansion," *IEEE Trans. Circuits Syst. Video Technol.*, vol. 13, no. 8, pp. 890–896, Aug. 2003.

[15] H. J. Kim, V. Sachnev, Y. Q. Shi, J. Nam, and H. G. Choo, "A novel difference expansion transform for reversible data embedding," *IEEE Trans. Inf. Forensics Security*, vol. 3, no. 3, pp. 456–465, Sep. 2008.

[16] Y. H. Chen, H. C. Huang, and C. C. Lin, "Block-based reversible data hiding with multi-round estimation and difference alteration," *Multimedia Tools and Applications*, 2015. (DOI: `10.1007/s11042-015-2825-9`)

[17] H. C. Huang, F. C. Chang, W. C. Fang, and T. H. Wang, "Reversible data hiding using enhanced prediction for progressive image transmission," *Proc. ICEIC'15*, pp. 180–181, 2015.

[18] H. C. Huang, T. H. Wang, and Y. Y. Lu, "Lossless data hiding with quadtree decomposition," *Proc. IIHMSP'13*, pp. 21–24, 2013.

[19] H. C. Huang, Y. Y. Lu, and Y. H. Chen, "Reversible data hiding with difference modification and rhombus relationships in quadtree decomposition," *Proc. IIHMSP'11*, pp. 13–16, 2011.

[20] C. F. Lee, H. L. Chen, and H. K. Tso, "Embedding capacity raising in reversible data hiding based on prediction of different expansion," *J. Systems and Software*, vol. 83, no. 10, pp. 1864–1872, Oct. 2010.

[21] H. C. Huang, I. H. Wang, and Y. Y. Lu, "High capacity reversible data hiding with adjacent-pixel-based difference expansion," *Proc. ICICIC'09*, pp. 639–642, 2009.

[22] H. C. Huang, Y. H. Chen, and I. H. Wang, "Reversible data hiding with improved histogram alteration method," *Proc. IIHMSP'10*, pp. 151–154, 2010.